Supplementary Information

Crystallinity-dependent enhancement of ionic conductivity on multi-interactive molecular materials

Gil Ryeong Lee, Hiroyoshi Ohtsu, Jin Young Koo, Yumi Yakiyama, Moon Jeong Park, Daishi Inoue, Daisuke Hashizume, and Masaki Kawano

Contents of Supplementary Information:

1: General Experimental Information

All chemicals were reagent grade and used as received. All reactions were performed at ambient temperature in air. The single crystal X-ray diffraction data for initial NH_4TPHAP-**A** and NH_4TPHAP-**B** were collected on an ADSC Quantum-210 detector with a synchrotron radiation ($\lambda =$ 0.750 or 0.700 Å) at 2D SMC beamline of the Pohang Accelerator Laboratory (PAL), Korea. The single crystal X-ray diffraction data for initial NaTPHAP-**B** were collected on a Bruker APEX II QUAZAR instrument in house. The X-ray powder diffraction data of initial NaTPHAP-**A** was collected on a diffractometer equipped with a blue imaging plate detector at BL19B2 beam line, SPring-8, Japan. The X-ray powder diffraction data of hydrated NH_4TPHAP-**A**, NaTPHAP-**A**, NH_4TPHAP-**B** and NaTPHAP-**B** were collected on a Bruker D8 ADVANCE using Cu $K\alpha_1$ radiation in house. Thermogravimetric (TG) analysis was carried out at a ramp rate of 10 K/min in a nitrogen flow (20 ml/min) with Scinco TGA N-1000. Elemental analyses were performed on an Elementar vario MICRO cube at Technical Support Center at Pohang University of Science and Technology.

2: Syntheses

Synthesis of ammonium 2,5,8-tri-(4-pyridyl)-1,3,4,6,7,9-hexaazaphenalenate, NH₄TPHAP

4-pyridylamidine hydrochloride (9.10 g, 57.7 mmol) and potassium tricyanomethanide (1.50 g, 11.6 mmol) were placed in a Teflon-lined stainless autoclave and heated at 200 ºC for 16 h.   At this stage, a NMR yield of the product is about 60%.   A 2M HCl aqueous solution was added to the reaction mixture.   And the aqueous layer was neutralized with a 30% ammonia aqueous solution. The resultant solid was purified by using MeCN to give single crystals (0.97 g, 37%). ^{1}H NMR (500 MHz, DMSO-d_6): δ 8.85 (d, 6H, J = 6 Hz), 8.45 (d, 6H, J = 6 Hz); elemental analysis calcd (%) for $C_{24.3}H_{30.8}N_{10}O_{5.1}$ (=$C_{22}H_{12}N_9(NH_4)(CH_3OH)_{2.3}(H_2O)_{2.8}$): C, 53.59; H, 5.70; N, 25.72. Found: C, 53.64; H, 5.48; N, 25.93.

Synthesis of sodium 2,5,8-tri-(4-pyridyl)-1,3,4,6,7,9-hexaazaphenalenate, NaTPHAP

Synthetic process is same as synthesis of NH₄TPHAP except for 5M NaOH aqueous solution instead of 30% ammonia aqueous solution for neutralization.   The resultant solid was collected and purified by using MeCN to give the brown powder (2.23 g, 43%). ^{1}H NMR (500 MHz, DMSO-d_6): δ 8.76 (d, 6H, J = 6 Hz), 8.39 (d, 6H, J = 6 Hz); elemental analysis calcd (%) for $C_{22}H_{22.4}N_9O_{5.2}Na$ (=$C_{22}H_{12}N_9Na(H_2O)_{5.2}$): C, 50.91; H, 4.35; N, 24.29. Found: C, 50.94; H, 4.23; N, 24.00.

Sample preparation of water resistive NH₄TPHAP-A

Single crystals of NH₄TPHAP-**A** were prepared by slow evaporation from NH₄TPHAP/MeOH solution (5.9 mM) at room temperature.   Needle shape pale brown crystals can be obtained within 1 day.

Sample preparation of water resistive NaTPHAP-A

Pale yellow crystalline powder of NaTPHAP-**A** was prepared by the vapour diffusion using MeOH solution of purified NaTPHAP (26.4 mM) and ethyl acetate for 3 days.   Detailed experimental setting is shown in Fig. S1a.

Sample preparation of non-water resistive NH$_4$TPHAP-B

Single crystals of NH$_4$TPHAP-**A** were prepared by slow evaporation from NH$_4$TPHAP/MeOH solution (3.4 mM) at room temperature.   Prism shape yellow crystals can be obtained in 6 hours.

Sample preparation of non-water resistive NaTPHAP-B

Single crystals of NaTPHAP-**B** were prepared by the vapour diffusion using MeOH solution of purified NaTPHAP (23.5 mM) and ethyl acetate with smaller scale for 1 day.   Detailed experimental setting is shown in Fig. S1b.

Sample preparation of hydrated TPHAP powders

Hydrated powder of NH$_4$TPHAP and NaTPHAP were prepared by keeping initial materials at 95% RH and 30 ºC for 12 hours in a sealed plastic container.   In order to keep the hydrated condition during XRPD measurements, we used a commercially available dorm type airtight cell (Bruker AXS) with additional water mist.   Transfer of the sample from the hydration container to the airtight cell was performed as quickly as possible.

3: Single crystal X-ray structure determination

Single Crystal X-ray Diffraction Analysis

All the structures were solved by direct methods (SHELXS-97/SHELXS-2014) and refined by full-matrix least squares calculations on F^2 (SHELXL-2014) using the SHELX-TL program.

X-ray Crystallographic data for initial NH$_4$TPHAP-A single crystal

$C_{22}H_{16}N_{10}O_{3.75}$, M_r = 480.45, crystal dimensions 0.50 × 0.01 × 0.01 mm^3, monoclinic, space group $C2/c$, a = 39.9667(3), b = 3.761 Å, c = 35.3988(4) Å, β = 122.88°, V = 4468.64(6) Å^3, Z = 8, ρ_{calcd} = 1.428 g cm^{-3}, μ = 1.15 cm^{-1}, λ = 0.750 Å (synchrotron radiation), T = 100(2) K, 3736 unique reflections out of 5108 with $I > 2\sigma(I)$, 439 parameters, 81 restraints, 2.152 < θ < 29.554°, final R factors $R1$ = 0.0496 and w$R2$ = 0.1369, GOF = 1.040. CCDC deposit number 1436932.

X-ray Crystallographic data for initial NH$_4$TPHAP-B single crystal

$C_{22.88}H_{19}N_{10}O_{0.87}$, M_r = 447.88, crystal dimensions 0.12 × 0.08 × 0.01 mm^3, tetragonal, space group $P42/n$, a = b = 21.6792(1) Å, c = 9.235 Å, V = 4340.34(4) Å^3, Z = 8, ρ_{calcd} = 1.371 g cm^{-3}, μ = 0.88 cm^{-1}, λ = 0.700 Å (synchrotron radiation), T = 100(2) K, 5779 unique reflections out of 6333 with $I > 2\sigma(I)$, 384 parameters, 0 restraints, 2.361 < θ < 29.529°, final R factors $R1$ = 0.0508 and w$R2$ = 0.1469, GOF = 1.023. CCDC deposit number 1436933.

X-ray Crystallographic data for initial NaTPHAP-B single crystal

$C_{27}H_{32}N_9NaO_5$, M_r = 585.60, crystal dimensions 0.25 × 0.03 × 0.03 mm^3, orthorhombic, space group $Pbcn$, a = 13.91(1) Å, b = 20.33(2) Å, c = 10.300(1) Å, V = 2912(6) Å^3, Z = 4, ρ_{calcd} = 1.336 g cm^{-3}, μ = 0.108 cm^{-1}, λ = 0.71073 Å (Mo Kα), T = 100(2) K, 1926 unique reflections out of 3002 with $I > 2\sigma(I)$, 228 parameters, 0 restraints, 1.774 < θ < 26.448°, final R factors $R1$ = 0.0485 and w$R2$ = 0.1055, GOF = 1.023. CCDC deposit number 1436931.

4: *ab Initio* XRPD crystal structure determination

X-ray powder structure analysis for initial NaTPHAP-A powder

$C_{22}N_9NaO_5$ M_r = 493.28, monoclinic, $P2_1/n$, a = 32.313(3) Å, b = 19.769(2) Å, c = 3.7343(3) Å, β = 98.59(1)°, V = 2358.7(4) Å^3, T = 300(2) K.   Details of powder analysis are described below.   CCDC deposit number 1436930.

High quality powder X-ray diffraction pattern of initial NaTPHAP-**A** was recorded at 300 K in transmission mode [0.3 mm capillary; synchrotron radiation λ = 1.3 Å; 2θ range, 0.01° to 78.08°; step size, 0.01°; data collection time, 50 min] with a blue IP detector (BL19B2, SPring-8).   The XRPD pattern of NaTPHAP-**A** was indexed using the program DICVOL (Boultif, A.; Louër, D. *J. Appl. Crystallogr*. **1991**, *24*, 987-993) to give a monoclinic unit cell (a = 32.32309 Å, b = 19.78106 Å, c = 3.73812 Å, β = 98.277°, V = 2365.200 Å^3) with good Figure of merit.   The space group was assigned from systematic absences as *P2₁/n*.   Unit cell and profile refinement were carried out using the Pawley method, led to good fit (χ^2 = 4.62) for these lattice parameters and space group.   Structure solution was carried out by the simulated annealing method with the program DASH (David, W. I. F.; Shankland, K; van de Streek, J; Pidcock, E; Motherwell, W. D. S.; Cole, J. C, *J. Appl. Crystallogr.,* **2006**, *39*, 910-915).   Four rigid groups; TPHAP in which $C_{HAPskelton}$-$C_{pyridyl}$, two Na$^+$ atoms and O (from water), in asymmetric unit and Z = 4 for space group *P2₁/n* were introduced by using a constrained Z-matrix description.   During annealing, 25 runs of 1 × 10^7 Monte Carlo moves each were performed.   The best structure obtained (Profile χ^2 = 12.18) was taken as the starting structural model for Rietveld refinement.

The Rietveld refinement of NaTPHAP-**A** was performed with the program RIETAN-FP (Izumi, F.; Momma, K. *Solid State Phenom.*, **2007**, *130*, 15-20) and VESTA (Momma, K.; Izumi, F. *J. Appl. Crystallogr.*, **2008**, *41*, 653-658).   Restraints but no constraints for all bond lengths were employed to maintain the molecular geometry.   Atomic displacement parameters were refined isotropically with

uniform values for TPHAP and separately refined for oxygen from water and sodium.

Final Rietveld refinement result: $a = 32.313(3)$ Å, $b = 19.769(2)$ Å, $c = 3.7343(3)$ Å, $\beta = 98.59(1)°$, $V = 2358.7(4)$ Å^3, $R_{wp} = 2.955\%$ ($R_e = 2.314\%$), $R_p = 2.243\%$, $R_B = 5.395\%$, $R_F = 4.361\%$; 4701 profile points (2θ range, 3 to 50°); 272 refined variables.   The refinement result is shown in Fig. S7.

5: Ionic conductivity measurement

The pellets for ionic conductivity measurement were prepared from ground powder of all materials with a mortar and a pestle.   The powders (35-40 mg) were put into a standard 13 mm die and pressed at 5 t for 1 minute.   The pellet thickness was ~0.2 mm.   The pellet shapes before and after hydration is shown in Fig. S8.

Ionic conductivities were measured with a home-built two-electrode cell with two stainless-steel blocking electrodes by a.c. impedance spectroscopy with a Princeton Applied Research Versa Stat 3 analyzer in the frequency range 100 Hz to 100 KHz at various humidity (60−95% RH) and 30 ºC after keeping the pellet under each condition for more than 12 h in a humidity controllable incubator. Impedance value was read at high-frequency plateau.   Examples are shown in Fig. S9.   Hydrated condition by deuterium oxide was prepared by keeping electrode at 95% RH and 30 ºC for 12 hours in a sealed plastic container.   All conductivity results were described in Table S1.

Arrhenius plots of all samples were calculated by temperature-dependent conductivity.   The obtained activation energy E_a were described in Table S2 and Fig S10.   We couldn't obtain E_a of NaTPHAP-**B** because the data didn't fit well by simple Arrhenius equation.   This results suggests that there are combination of vehicle mechanism of Na$^+$ or NH$_4^+$ and Grotthuss mechnism of proton. However, it is difficult to make a clear conclusion because water contents of each condition were not unified.

Relative humidity (% RH)	Conductivity (S·cm^{-1})			
	NaTPHAP-**A**	NH$_4$TPHAP-**A**	NaTPHAP-**B**	NH$_4$TPHAP-**B**
70	5.96×10^{-6}	4.00×10^{-7}	-	-
75	1.44×10^{-5}	6.37×10^{-7}	1.63×10^{-7}	2.01×10^{-7}
80	4.70×10^{-5}	2.17×10^{-6}	3.21×10^{-7}	9.71×10^{-7}
85	1.65×10^{-4}	5.63×10^{-6}	8.26×10^{-7}	2.67×10^{-6}
90	7.28×10^{-4}	1.88×10^{-5}	2.75×10^{-6}	7.04×10^{-6}
95	5.92×10^{-3}	2.79×10^{-3}	3.17×10^{-5}	4.65×10^{-5}
95 (using D$_2$O)	9.77×10^{-4}	2.95×10^{-3}	1.29×10^{-5}	2.23×10^{-5}

Table S1. Conductivity results of TPHAP powders.

Relative humidity (% RH)	Activation energy (eV)			
	NaTPHAP-**A**	NH$_4$TPHAP-**A**	NaTPHAP-**B**	NH$_4$TPHAP-**B**
85	0.49(7)	0.31(1)	-	-
95	0.20(2)	0.30(8)	-	1.26(14)

Table S2. Activation energy of TPHAP powders.

6: Evaluation of ionic interaction energy in A-phases

Evaluation of ionic interaction energy in **A**-phases were performed by DFT calculation using Gaussian 09W program (Gaussian, Inc., Wallingford, CT, 2009) at M06-2X/6-311G** level based on crystal structures. The two types of interactions of TPHAP$\cdots$NH$_4^+$ and TPHAP$\cdots$Na$^+$, and their energies were shown in the right and Table S3. The interactions of TPHAP$^-$ with Na$^+$ are much stronger than with NH$_4^+$. However, the
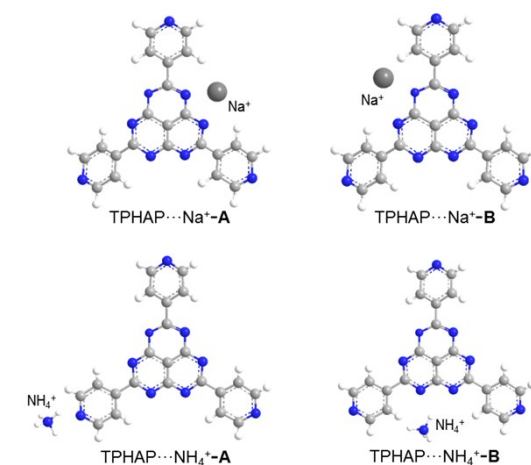
Positions of the ions in each condition for DFT calculation.

number of the effective interactions are totally different per TPHAP$^-$ (TPHAP$^-\cdots$Na$^+$-**A** $\times$ 1, TPHAP$^-\cdots$Na$^+$-**B** $\times$ 1, TPHAP$^-\cdots$NH$_4^+$-**A** $\times$ 3, TPHAP$^-\cdots$NH$_4^+$-**B** $\times$ 1 (from crystal structures)) resulting in the higher stabilization energy in NH$_4$TPHAP-**A**. This might be the one of the reason of smaller conductivity of NH$_4$TPHAP-**A** than NaTPHAP-**A** dispite larger mobility of NH$_4$TPHAP-**A**.

	E (RM062X) (A.U.)	E_{int} (kcal/mol)
TPHAP$^-$ (in Na$^+$ system)	−1338.067677	
TPHAP$^-$ (in NH$_4^+$ system)	−1338.028112	
Na$^+$	−162.0501367 (position A, B)	
NH$_4^+$	−56.86514347 (position A) −56.88024149 (position B)	
TPHAP$\cdots$Na$^+$-**A**	−1500.255337	−86.29717346
TPHAP$\cdots$Na$^+$-**B**	−1500.248943	−82.28507852
TPHAP$\cdots$NH$_4^+$-**A**	−1394.971553	−49.13257894
TPHAP$\cdots$NH$_4^+$-**B**	−1395.024541	−72.90894584

Table S3. Interaction energy between TPHAP$^-$ and Na$^+$ or NH$_4^+$ (M06-2X/6-311G**).

In addition, we evaluated the interactions between water and NH$_4^+$ or Na$^+$ by ab initio calculation (MP2/6-311G). The results clearly showed the larger stabilization energy between Na$^+$ and water

than that between NH_4^+ and water (Table S4).   From these results, the conductivity differences in both of the systems can be explained by that the larger interaction with water of Na^+ enabled the quicker adsorption of water within the system than that of NH_4^+.   On the contrary, the stronger total coulombic interaction with the framework and the smaller interaction with water of NH_4^+ system resulted in preventing the quick water adsorption to the network.   It is impossible at this moment to make conclusion about the total stabilization energy and the conductivity features of the two systems because such simple discussions using the calculation only based on the hydrogen bonding and coulombic pair (TPHAP and ions) structures are insufficient. Even though, these results reasonably explain the ionic conductivity features of the **A**-phase networks.

	E (RHF) (A.U.)	E_{int} (kcal/mol)
Na^+	−161.664232886	—
NH_4^+	−56.5584458548	—
H_2O	−76.0467175244	—
$H_2O \cdots Na^+$	−237.754377036	−27.25062
$H_2O \cdots NH_4^+$	−132.639713014	−21.68022

Table S4: Hydrogen bonding interaction energy between water and Na^+ or NH_4^+ (MP2/6-311G).

7: Figures
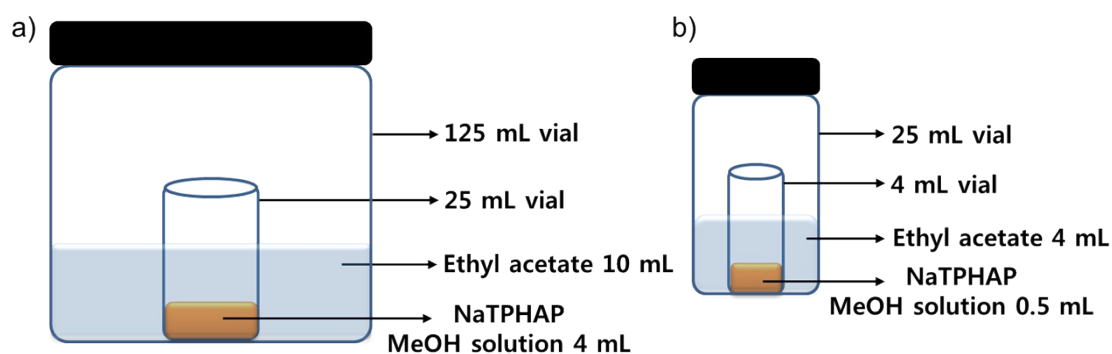
Figure S1. Experimental condition of NaTPHAP crystallization. a) For the preparation of crystalline powder of NaTPHAP-**A**. b) For the preparation of single crystal of NaTPHAP-**B**.

N1A$\cdots$N2(HAP) : 2.8910(18) Å

N2A$\cdots$N4(HAP) : 3.485(4) Å

N2A$\cdots$N6(HAP) : 2.990(4) Å
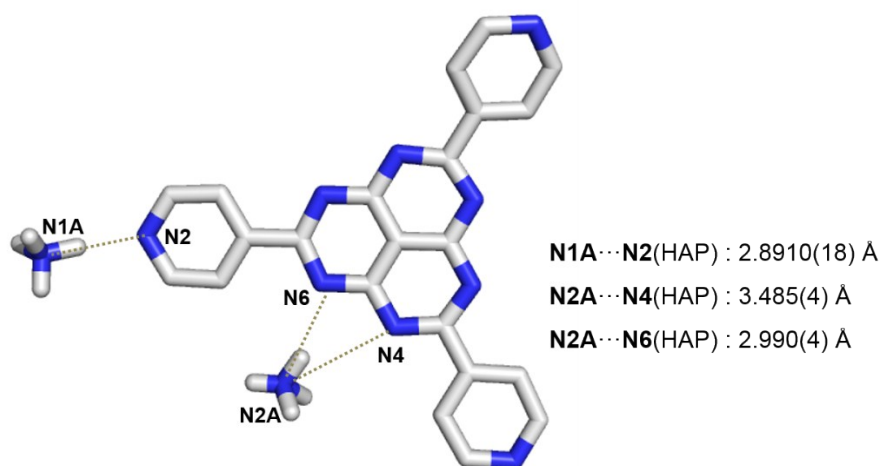
Figure S2. Bond distances between NH_4^+ and $TPHAP^-$ in NH_4TPHAP-**A**.

Na$^+$32$\cdots$N3(HAP) : 3.0(2) Å

Na$^+$32$\cdots$N4(HAP) : 3.0(2) Å

Na$^+$33$\cdots$N11(HAP) : 3.6(2) Å

Na$^+$33$\cdots$N12(HAP) : 3.1(2) Å

Figure S3. Bond distances between Na^+ and $TPHAP^-$ in NaTPHAP-**A**.

N1A···N31(HAP) : 3.1891(14) Å

N1A···N32(HAP) : 2.9871(14) Å

N1A···N35(HAP) : 2.9957(14) Å

N1A···N36(HAP) : 3.1745(14) Å

Figure S4. Bond distances between NH_4^+ and TPHAP$^-$ in NH$_4$TPHAP-**B**.

Na$^+$···N3 (HAP) : 2.592(3) Å
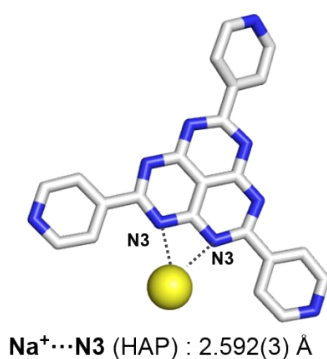
Figure S5. Bond distance between Na$^+$ and TPHAP$^-$ in NaTPHAP-**B**.

A: 5.0 Å × 4.0 Å, **D**: 4.0 Å × 3.5 Å
B: 4.2 Å × 4.0 Å, **E**: 5.0 Å × 3.0 Å
C: 5.0 Å × 2.5 Å

A~E: 4.1 Å × 2.8 Å
F: 4.3 Å × 5.9 Å
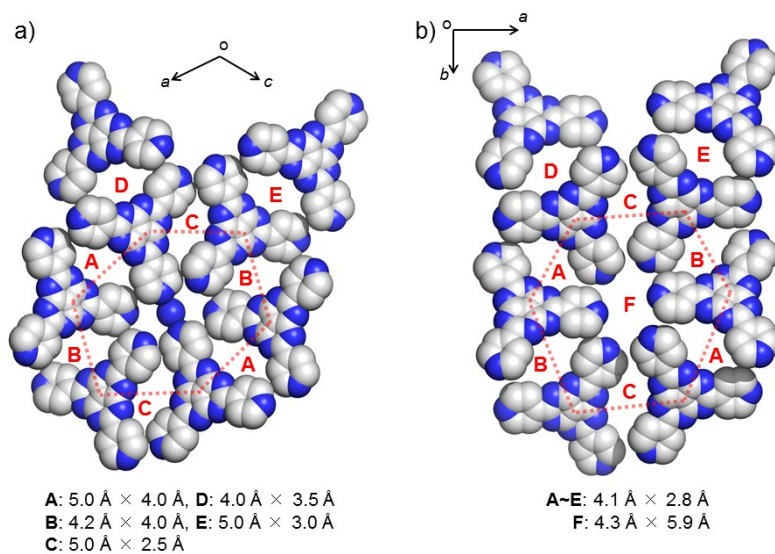
Figure S6. Pore size in each structure. a) NH$_4$TPHAP-**A**, b) NaTPHAP-**A**.

Monoclinic　　P2$_1$/n
a = 31.3133(29) Å , b = 19.7689(16) Å ,
c = 3.7342(3) Å , β = 98.59(1) °,
V = 2358.7(4) Å³,
λ = 1.3 Å,　　　RT

R$_{wp}$ = 2.96 %, R$_B$ = 5.40 %, R$_F$ = 4.36 %
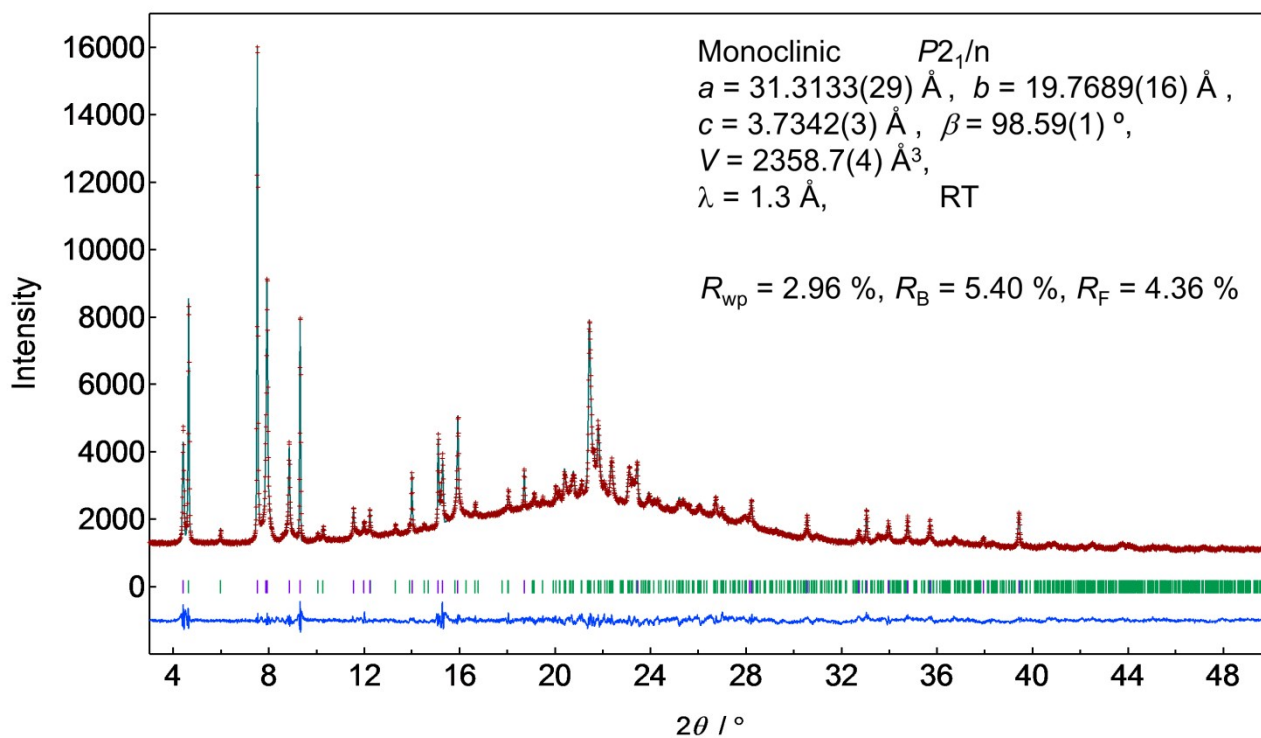
Figure S7. Experimental (red), calculated (black), and difference (blue) XRPD profiles from the final Rietveld refinement of initial NaTPHAP-**A**.
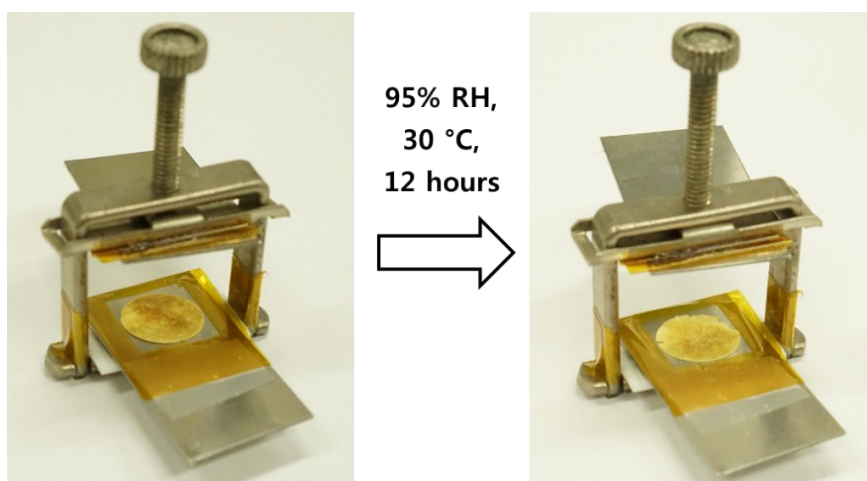
95% RH,
30 °C,
12 hours

Figure S8. Pellet shapes of TPHAP powders before and after hydration.
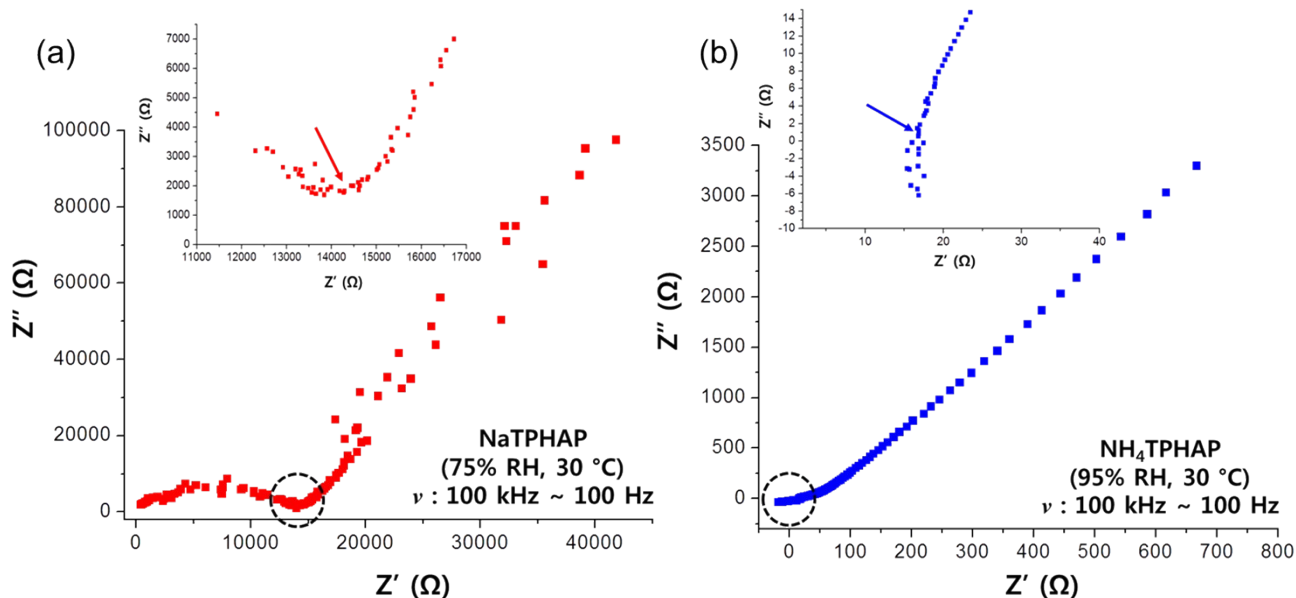
Figure S9. Examples of Nyquist plots. a) NaTPHAP-**A** at 75% RH, 30 °C, b) NH₄TPHAP-**A** at 95% RH, 30 °C. Inset figure shows the magnified plot of the region encircled with dotted line.
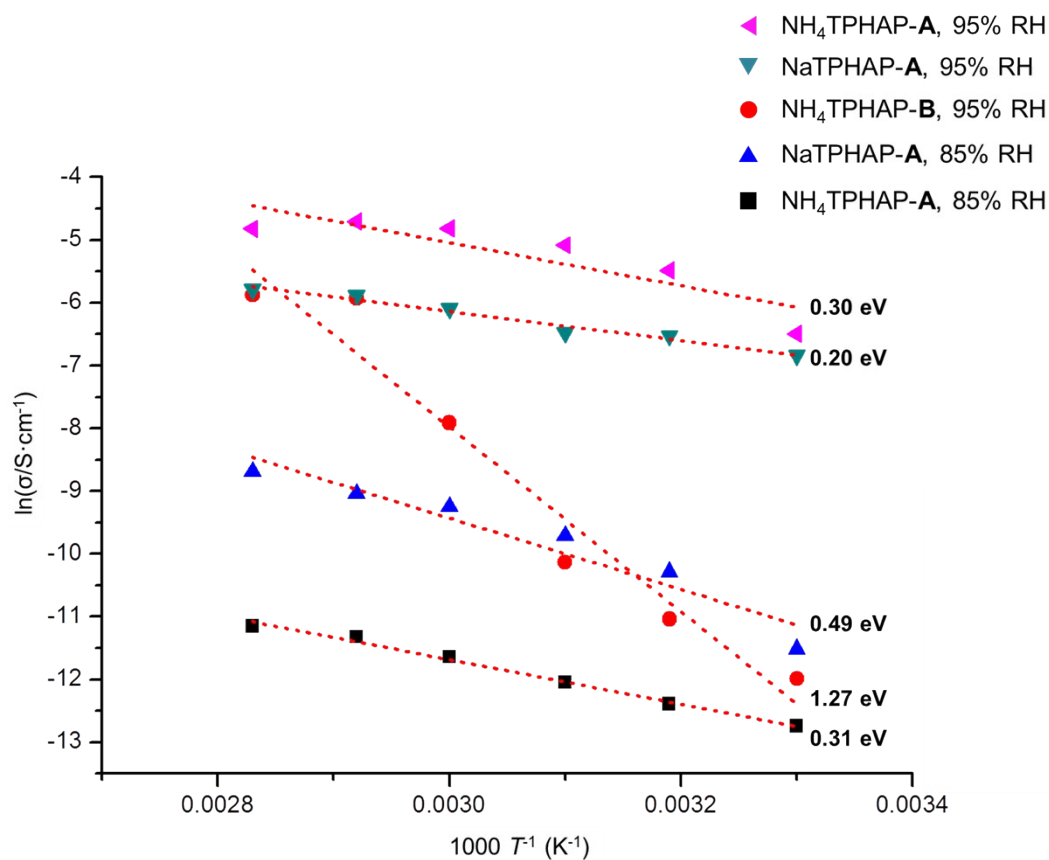
Figure S10. Arrhenius plots of TPHAP powders.
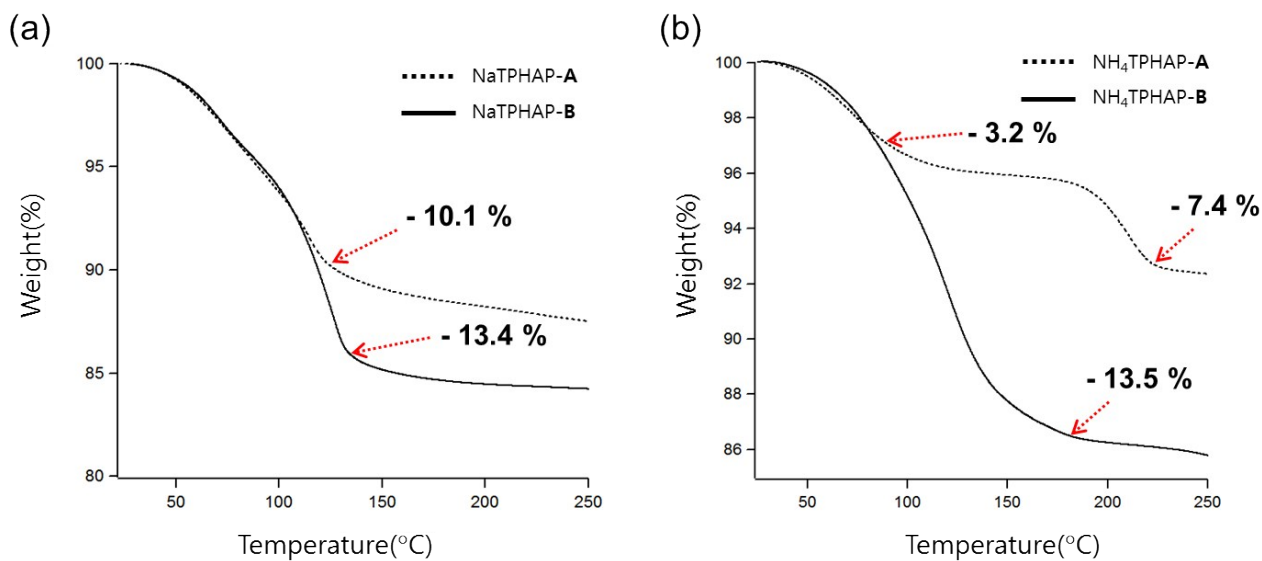
Figure S11. TG plots of NaTPHAP and NH$_4$TPHAP initial powders; **A** phases (dotted), **B** phases (black).   a) NaTPHAP powders, b) NH$_4$TPHAP powders.
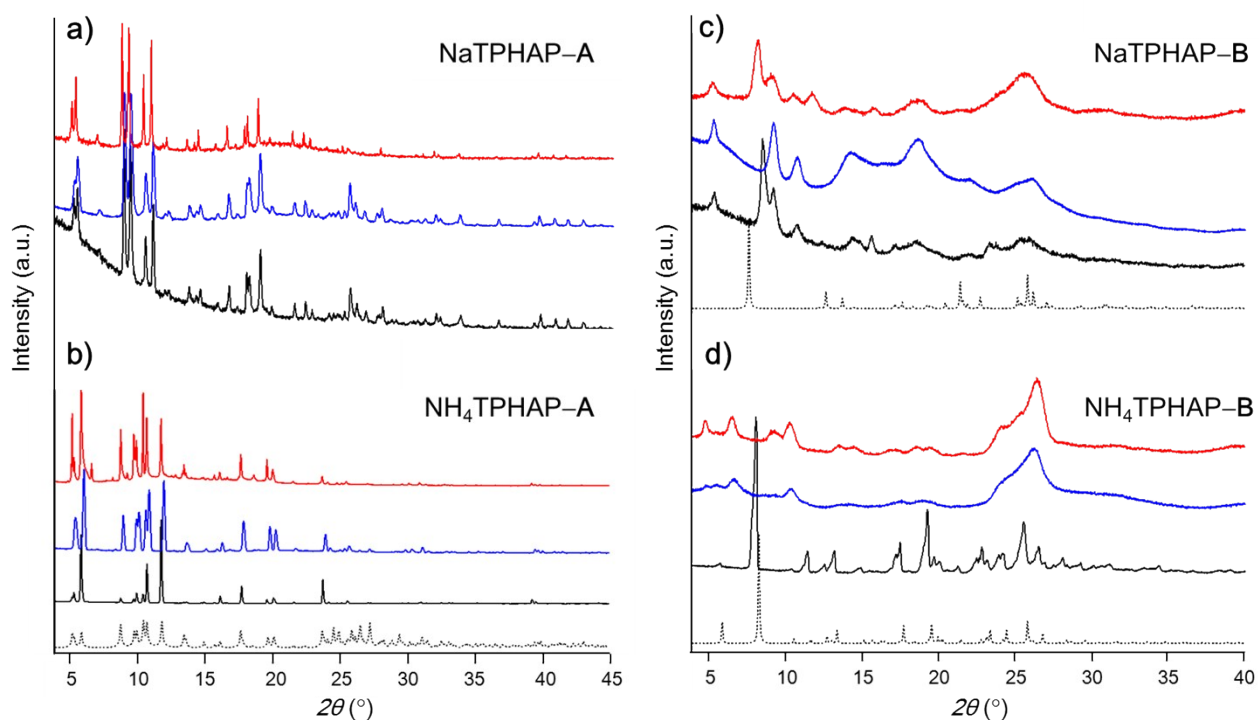
Figure S12.   XRPD patterns of NaTPHAP and NH$_4$TPHAP powders.   Simulated patterns (dotted), initial powder (black), hydrated powder (blue) and dried powder (red).   a) NaTPHAP-**A**, b) NH$_4$TPHAP-**A**, c) NaTPHAP-**B**, d) NH$_4$TPHAP-**B**.